Prediction of Apollo Service Module Motion after Jettison

D. H. MERCHANT* AND R. M. GATES†
The Boeing Company, Houston, Texas

AND

J. F. MURRAY‡
Boeing Computer Services Inc., Houston, Texas

After the re-entry separation during two Apollo missions, the astronauts observed the jettisoned Service Module to be moving in the opposite direction from that of the initial separation. This anomalous retrograde motion was attributed to the gross reorientation of the residual Service Module propellants. To determine analytically the effects of propellant reorientation on Service Module dynamics after jettison, an analytical representation and computer program were developed to simulate the complex interaction between the spacecraft motion and the general motion of the fluids within the propellant tanks. The resulting numerical analyses indicated that forces exerted on the tanks by the sloshing propellants can combine with unsymmetric thrust forces to produce the unexpected retrograde motions observed during the Apollo missions.

Nomenclature

$\mathbf{A}_0$ = rigid-body component of a propellant mass acceleration defined by Eqs. (3–5)
$\mathbf{A}_p$ = translational inertial acceleration of a propellant mass
C_F = proportionality constant in friction force expressions
$\mathbf{e}_R, \mathbf{e}_M, \mathbf{e}_T$ = radial, meridional, and tangential unit vectors associated with a local spherical coordinate system
$\mathbf{F}$ = total force applied to SM centroid in SM body-fixed coordinate system
$\mathbf{F}_p$ = force applied to a propellant mass when in contact with tank wall
$\tilde{I}_s$ = inertia tensor of SM exclusive of sloshing propellant
$\mathbf{M}$ = total moment applied to SM centroid in SM body-fixed coordinate system
M_p = mass of a sloshing propellant
M_s = mass of SM exclusive of sloshing propellant
$\mathbf{R}_0$ = position vector of origin of a local coordinate system relative to SM centroid
$\mathbf{R}_p$ = position vector of a propellant mass relative to SM centroid
$\mathbf{r}_p$ = position vector of a propellant mass relative to origin of local coordinate system
R_T = radius of propellant tank cylinder and hemisphere
SM = Service Module
$\tilde{T}_{BI}$ = Euler transformation from SM body-fixed to inertial coordinate system
$\ddot{\mathbf{X}}$ = translational inertial acceleration of SM centroid
α = angle between the rotational velocity vector and the body-fixed x axis
β = angle between the inertial X axis and the body-fixed x axis
ρ, θ, ϕ = relative radial position, meridional angle, and tangential angle, respectively, of a propellant mass in a local spherical coordinate system
ρ_C, η_C, ϕ = relative radial position, longitudinal position, and tangential angle, respectively, of a propellant mass in a local cylindrical coordinate system
Ω = rotational inertial velocity of SM centroid

Subscripts

CR, CL, CT = radial, longitudinal, and tangential components of a vector in a local cylindrical coordinate system
R, M, T = radial, meridional, and tangential components of a vector in a local spherical coordinate system

Introduction

THE Service Module (SM) is 13 ft long and 12.8 ft in diameter. It provides power and propulsion for the Apollo Command Module (CM) throughout each mission. Prior to normal re-entry of the CM, the SM is jettisoned. Since the SM does not have closed-loop attitude control in the jettison mode, a preset firing sequence of the SM Reaction Control System (RCS) thrusters is intended to provide adequate and predictable SM/CM separation. The RCS firing sequence used for the Apollo flights through Apollo 12 specified translational thrust along the SM longitudinal axis until fuel depletion (about 300 sec) with the roll jets firing for 5.5 sec after separation to provide spin stability. For the missions of Apollo 7–11, flight data have shown that the actual separation velocity was much less than expected.[1,2] More-

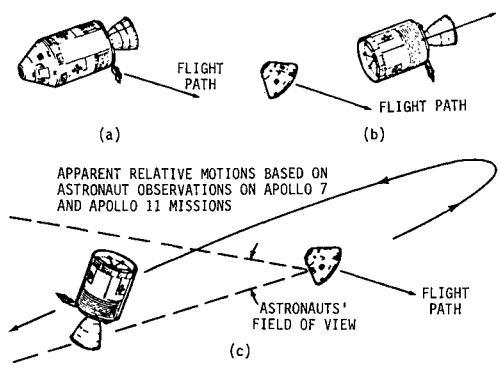

Fig. 1 Command module/service module separation.

Presented as Paper 70-1047 at the AAS/AIAA Astrodynamics Conference, Santa Barbara, Calif., August 19–21, 1970; submitted September 18, 1970; revision received February 17, 1971. This work was supported by the National Aeronautics and Space Administration under Contract NASw 9-1650.

* Specialist Engineer, Structures & Dynamics, Aerospace Group. Member AIAA.

† Senior Engineer, Structures & Dynamics, Aerospace Group Member AIAA.

‡ Senior Systems Analyst, Southeast Division. Associate Member AIAA.

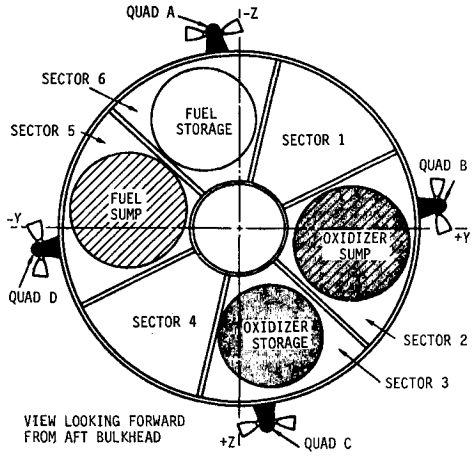

Fig. 2 Service module tanks and RCS quads.

over, during the flights of Apollo 7 and 11, the crew reported sighting the SM tumbling after jettison. If the SM remains stable throughout the jettison maneuver, it will neither tumble nor enter the crew's field of vision. These two sightings indicate primarily that the SM attained a retrograde velocity relative to the CM (Fig. 1).

The anomalous motion of the SM was attributed to the gross longitudinal sloshing of the residual Service Propulsion System (SPS) propellants within the sump tanks.[2,3] The four tanks are arranged as shown in Fig. 2. At the time of SM jettison, the storage tanks are empty, and the sump tanks contain the residual oxidizer and fuel. The reorientation of the propellants can produce major disturbing forces, since they comprise as much as 25% of the total SM weight. The mass-spring slosh analogy commonly used to represent the sloshing of fluids is not applicable for this phenomenon, since the fluid is essentially in a low-g environment of variable magnitude. Furthermore, since the residual propellant typically occupies less than 15% of the tank volume, the fluid undergoes completely general motion within the tank.

This paper describes a) an analytical simulation of the complex interaction between the spacecraft motion and the fluid motion inside the tanks and b) the results of a numerical simulation which indicate that the observed retrograde motions can be reproduced analytically. These results, along with additional data presented in Ref. 4, formed the basis for a decision by the NASA Manned Spacecraft Center to eliminate the possibility of SM retrograde motions by modifying the RCS timing sequence. References 5 and 6 describe the theoretical derivations and the digital computer program developed for the SM jettison studies.

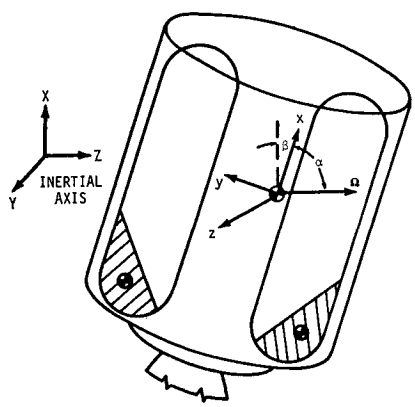

Fig. 3 Service module coordinate systems and orientation angles.

Theoretical Development

The SM with sloshing residual propellants is idealized as a 3-mass system having 12 dynamic degrees of freedom. Three translational and 3 rotational freedoms represent the rigid-body motion of the SM, and 3 translational freedoms represent the general motion of each propellant centroid within its tank. The propellants are idealized as perfectly inelastic point masses which move within approximate envelopes defined by the fluid centroidal positions. When either of the propellant masses contacts the boundary surface of its idealized tank, a constraint force normal to the surface is imparted to the propellant mass in addition to friction forces tangential to the boundary surface. The equal and opposite reactions are then applied to the SM centroid as external forces and moments. Additional external forces and moments result from the RCS thruster firings.

The 3-dimensional motion of the SM centroid under the influence of the RCS thrust and propellant reaction forces is described in an inertial coordinate system. The forces applied to the SM centroid and the general motions of the propellant point masses relative to the rigid SM are described in a moving coordinate system fixed at the SM centroid. These coordinate systems, shown in Fig. 3, are related by orthogonal Euler angle transformations. For simplicity in studying the complex interaction between the spacecraft dynamics and propellant motions, centrifugal forces arising from the slight curvature of the Apollo re-entry trajectory are assumed to be exactly equilibrated by the earth's gravitational forces. The equations of motion are therefore developed without reference to the earth's gravitational field.

To aid in understanding the SM dynamics during jettison as determined by the numerical simulations, two SM orientation angles are defined (see Fig. 3): α is the angle between the SM body-fixed longitudinal axis (x) and the rotational velocity vector ($\boldsymbol{\Omega}$); β is the angle between the body-fixed x axis and the longitudinal axis (X) of the inertial coordinate system. When the SM is spin stabilized, $\alpha \simeq 0$; when the SM is tumbling, $\alpha \to 90°$; and when $\beta > 90°$, the SM is tending to return to its initial position.

The translational acceleration of the SM centroid is given in the inertial coordinate system by

$$\ddot{\mathbf{X}} = (\tilde{T}_{BI})\mathbf{F}/M_S \tag{1}$$

The rotational acceleration of the SM centroid is given in the body-fixed coordinate system by Euler's equations of motion:

$$\dot{\boldsymbol{\Omega}} = \check{I}_S^{-1}(\mathbf{M} - \boldsymbol{\Omega} X \check{I}_S \boldsymbol{\Omega}) \tag{2}$$

The total forces and moments applied to the SM centroid in Eqs. (1) and (2) result from the RCS thrust forces required by the evasive jettison maneuver and from the propellant mass reaction forces generated whenever the propellants contact the tank walls. The translational inertial acceleration of each propellant mass is given in the SM body-fixed coordinate system by

$$\mathbf{A}_p = \mathbf{F}/M_s + \dot{\boldsymbol{\Omega}} X \mathbf{R}_p + \boldsymbol{\Omega} X \boldsymbol{\Omega} X \mathbf{R}_p + 2\boldsymbol{\Omega} X \dot{\mathbf{R}}_p + \ddot{\mathbf{R}}_p \tag{3}$$

Since the necessary equations of constraint for the propellant point masses may be most conveniently expressed in terms of local coordinate systems, Eq. (3) must be transformed from the SM body-fixed coordinate system. The three local coordinate systems used to describe the motion in each tank are shown in Fig. 4 along with the SM body-fixed coordinate system. Motions in the forward and aft hemispheres of each tank are described by two distinct spherical (ρ,θ,ϕ) coordinate systems whereas motion in the center of each tank is described by a cylindrical (ρ_C,η_C,ϕ) coordinate system. Transformations between the coordinate axes are facilitated by the fact that all the coordinate systems used in the analytical repre-

sentation (except the Euler system) are right-handed and orthogonal.

The propellant acceleration of Eq. (3) may be expressed as follows when the point mass is located in either the forward or the aft tank hemispheres. Since the SM is assumed to be rigid, the relative position, velocity, and acceleration are given by

$$\mathbf{R}_p = \mathbf{R}_0 + \mathbf{r}_p \qquad \dot{\mathbf{R}}_p = \dot{\mathbf{r}}_p \qquad \ddot{\mathbf{R}}_p = \ddot{\mathbf{r}}_p \quad (4)$$

Substituting these relations into Eq. (3) yields

$$\mathbf{A}_p = \mathbf{A}_0 + \dot{\boldsymbol{\Omega}}X\mathbf{r}_p + \boldsymbol{\Omega}X\boldsymbol{\Omega}X\mathbf{r}_p + 2\boldsymbol{\Omega}X\dot{\mathbf{r}}_p + \ddot{\mathbf{r}}_p \quad (5)$$

where $\mathbf{A}_0$ is the sum of all terms not depending on the relative propellant motion. The orthogonal components of relative position, velocity, and acceleration in the spherical coordinate system are readily obtained:[7]

$$\mathbf{r}_p = \rho\cdot\mathbf{e}_R \quad (6)$$

$$\dot{\mathbf{r}}_p = \dot{\rho}\cdot\mathbf{e}_R + \rho\cdot\dot{\theta}\cdot\mathbf{e}_M + \rho\cdot\dot{\phi}\cdot\sin\theta\cdot\mathbf{e}_T \quad (7)$$

$$\ddot{\mathbf{r}}_p = (\ddot{\rho} - \rho\cdot\dot{\theta}^2 - \rho\cdot\dot{\phi}^2\cdot\sin^2\theta)\cdot\mathbf{e}_R + (\rho\cdot\ddot{\theta} + 2\cdot\dot{\rho}\cdot\dot{\theta} - \rho\cdot\dot{\phi}^2\cdot\sin\theta\cdot\cos\theta)\cdot\mathbf{e}_M + (\rho\cdot\ddot{\phi}\cdot\sin\theta + 2\dot{\rho}\cdot\dot{\phi}\cdot\sin\theta + 2\rho\cdot\dot{\phi}\cdot\dot{\theta}\cdot\cos\theta)\mathbf{e}_T \quad (8)$$

The radial, meridional, and tangential components of the remaining terms of Eq. (5) may be simply obtained through the orthogonal transformation from the SM body-fixed coordinate system to the local spherical coordinate system. The scalar components, in the spherical coordinate system, of the inertial acceleration of a propellant mass located in either the forward or aft tank hemispheres are then expressed as follows:

$$(A_p)_R = (A_0)_R - (\Omega_M^2 + \Omega_T^2)\cdot\rho + 2\Omega_M\cdot\rho\cdot\dot{\phi}\cdot\sin\theta - 2\Omega_T\cdot\rho\cdot\dot{\theta} + \ddot{\rho} - \rho\cdot\dot{\theta}^2 - \rho\cdot\dot{\phi}^2\cdot\sin^2\theta \quad (9)$$

$$(A_p)_M = (A_0)_M + \dot{\Omega}_T\cdot\rho + \Omega_R\cdot\Omega_M\cdot\rho + 2\Omega_T\cdot\dot{\rho} - 2\Omega_R\cdot\rho\cdot\dot{\phi}\cdot\sin\theta + \rho\cdot\ddot{\theta} + 2\dot{\rho}\cdot\dot{\theta} - \rho\cdot\dot{\phi}^2\cdot\sin\theta\cdot\cos\theta \quad (10)$$

$$(A_p)_T = (A_0)_T - \dot{\Omega}_M\cdot\rho + \Omega_R\cdot\Omega_T\cdot\rho + 2\Omega_R\cdot\rho\cdot\dot{\theta} - 2\Omega_M\cdot\dot{\rho} + \rho\cdot\ddot{\phi}\cdot\sin\theta + 2\dot{\rho}\cdot\dot{\phi}\cdot\sin\theta + 2\rho\cdot\dot{\phi}\cdot\dot{\theta}\cdot\cos\theta \quad (11)$$

These general equations are applicable for either of two propellants located in either the forward or aft hemispheres.

The inertial acceleration of a propellant mass located in the cylindrical portion of a tank may be derived in an exactly analogous manner. The radial, longitudinal, and tangential components in the cylindrical coordinate system are as follows:

$$(A_p)_{CR} = (A_0)_{CR} - \dot{\Omega}_{CT}\cdot\eta_C - (\Omega_{CL}^2 + \Omega_{CT}^2)\cdot\rho_C + \Omega_{CR}\cdot\Omega_{CL}\cdot\eta_C + 2\Omega_{CL}\cdot\rho_C\cdot\dot{\phi} - 2\Omega_{CT}\cdot\dot{\eta}_C + \ddot{\rho}_C - \rho_C\cdot\dot{\phi}^2 \quad (12)$$

$$(A_p)_{CL} = (A_0)_{CL} + \dot{\Omega}_{CT}\cdot\rho_C + \Omega_{CR}\cdot\Omega_{CL}\cdot\rho_C - (\Omega_{CR}^2 + \Omega_{CT}^2)\cdot\eta_C + 2\Omega_{CT}\cdot\dot{\rho}_C - 2\Omega_{CR}\cdot\rho_C\cdot\dot{\phi} + \ddot{\eta}_C \quad (13)$$

$$(A_p)_{CT} = (A_0)_{CT} - \dot{\Omega}_{CL}\cdot\rho_C + \dot{\Omega}_{CR}\cdot\eta_C + \Omega_{CR}\cdot\Omega_{CT}\cdot\rho_C + \Omega_{CL}\cdot\Omega_{CT}\cdot\eta_C - 2\Omega_{CL}\cdot\dot{\rho}_C + 2\Omega_{CR}\cdot\dot{\eta}_C + \rho_C\cdot\ddot{\phi} + 2\dot{\rho}_C\cdot\dot{\phi} \quad (14)$$

When a propellant mass in a tank is floating free of its tank wall, the inertial acceleration ($\mathbf{A}_p$) is zero. For a propellant mass located in the forward or aft hemispheres, Eqs. (9–11) may be solved, respectively, for $\ddot{\rho}$, $\ddot{\theta}$, and $\ddot{\phi}$. The scalar second derivatives ($\ddot{\rho},\ddot{\theta},\ddot{\phi}$) may be successively integrated to obtain position and velocity relative to the SM centroid. Similarly, Eqs. (12–14) may be solved for $\ddot{\rho}_C$, $\ddot{\eta}_C$, and $\ddot{\phi}$ when a propellant is located in the cylindrical portion of its tank.

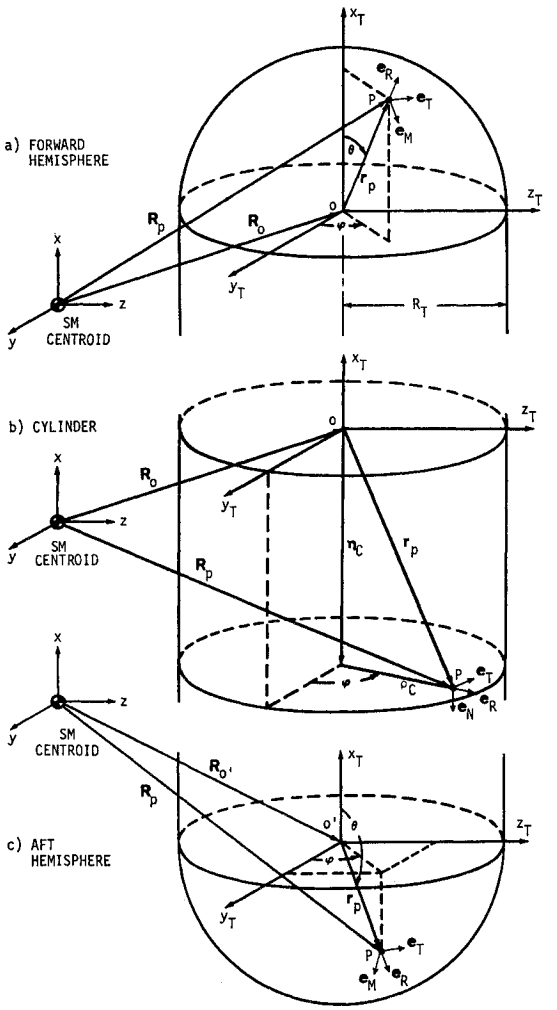

Fig. 4 Local tank coordinate systems.

When a propellant mass is in contact with its tank wall, a force of constraint normal to the boundary surface is applied to the mass. The kinematic constraint relations corresponding to the propellant mass in contact with its tank boundary surface are as follows:

$$\rho = R_T \qquad \dot{\rho} = \ddot{\rho} = 0 \quad (15)$$

The normal constraint force applied to a propellant mass by its tank hemisphere wall is simply the product of the mass times the radial acceleration Eq. (9) constrained by the kinematic relations of Eq. (15):

$$(F_p)_R = M_p[(A_0)_R - (\Omega_M^2 + \Omega^2)\cdot R_T + 2\Omega_M\cdot R_T\cdot\dot{\phi}\cdot\sin\theta - 2\Omega_T\cdot R_T\cdot\dot{\theta} - R_T\cdot\dot{\theta}^2 - R_T\cdot\dot{\phi}^2\cdot\sin^2\theta] \quad (16)$$

The normal force applied by a tank cylinder wall is obtained similarly from Eqs. (12) and (15) as

$$(F_p)_{CR} = M_p[(A_0)_{CR} - \dot{\Omega}_{CT}\cdot\eta_C - (\Omega_{CL}^2 + \Omega_{CT}^2)\cdot R_T + \Omega_{CR}\cdot\Omega_{CL}\cdot\eta_C + 2\Omega_{CL}\cdot R_T\cdot\dot{\phi} - 2\Omega_{CT}\cdot\dot{\eta}_C - R_T\cdot\dot{\phi}^2] \quad (17)$$

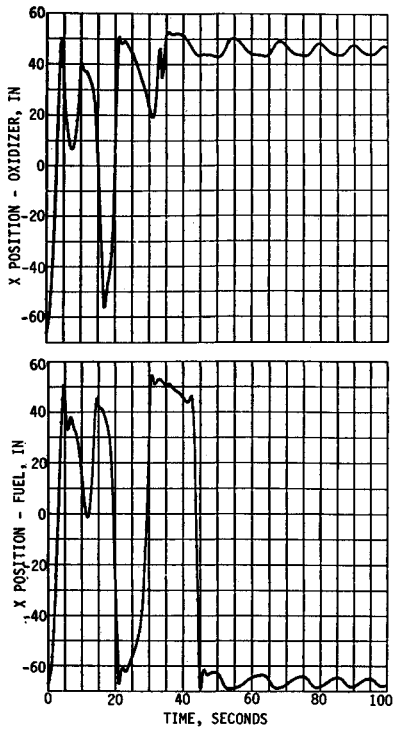

Fig. 5 Longitudinal positions of oxidizer and fuel.

The friction forces between a propellant and its tank wall are approximated by an empirical function proportional to the product of the radial force times the relative velocity. When a point mass is located in either hemisphere of its tank, the meridional and tangential components of the friction force applied to the propellant mass are given by

$$(F_p)_M = C_F \cdot R_T \cdot \dot{\theta} \cdot (F_p)_R \tag{18}$$

$$(F_p)_T = C_F \cdot R_T \cdot \dot{\phi} \cdot \sin\theta \cdot (F_p)_R \tag{19}$$

Note that the friction forces always oppose the relative motion since the normal force is negative whenever the propellant is in contact with the wall surface. When a point mass is located in the cylindrical portion of its tank, the longitudinal and tangential components of the friction force applied to the propellant mass are given by

$$(F_p)_{CL} = C_F \cdot \dot{\eta}_C \cdot (F_p)_{CR} \tag{20}$$

$$(F_p)_{CT} = C_F \cdot R_T \cdot \dot{\phi} \cdot (F_p)_{CR} \tag{21}$$

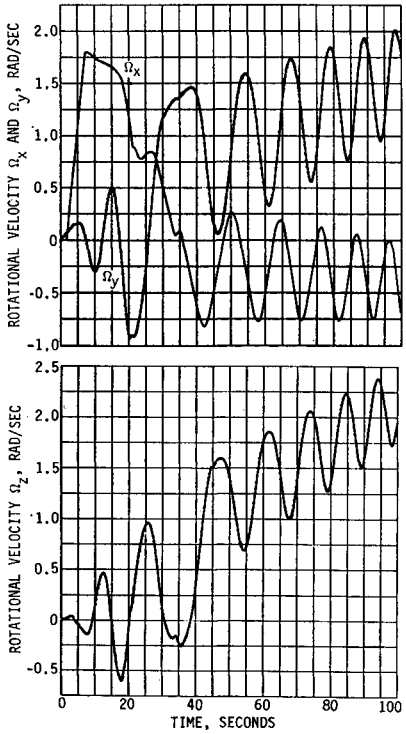

Fig. 6 Service module rotational velocities, Ω_x, Ω_y, and Ω_z.

For a propellant mass in contact with its forward or aft tank hemispheres, Eqs. (10) and (18) and Eqs. (11) and (19) may be combined with the kinematic constraint relations [Eq. (15)] to yield expressions for $\ddot{\theta}$ and $\ddot{\phi}$. Similarly, when a propellant mass is in contact with its tank cylinder, Eqs. (13) and (20) and Eqs. (14) and (21) may be combined with the constraint relations to yield expressions for $\ddot{\eta}_C$ and $\ddot{\phi}$. The relative positions and velocity of a propellant mass in contact with its tank boundary surface may be obtained by successively integrating these scalar second derivatives.

The changes of variables which occur as a propellant mass moves from the cylindrical section of a tank to a hemispherical section are effected by continuity equations. These equations, derived simply from the position expressions in local coordinates and their scalar time derivatives, provide continuous propellant motions across the tank section boundaries.

When either of the propellant masses contacts the boundary surface of its idealized tank, additional forces and moments are applied to the SM centroid. These additional propellant reaction forces are obtained by first reversing the direction of the forces defined by Eqs. (16–21) and then transforming them from the local coordinates into the SM body–fixed coordinate system. These reaction forces and the corresponding moments are then used in Eqs. (1) and (2) to yield SM rigid-body accelerations. However, as shown in Eq. (5), the SM rigid-body accelerations are themselves major contributions to the propellant accelerations and therefore to the propellant/spacecraft interaction forces. This nonlinear feature of the equations of motion is very significant to the numerical simulation of the jettison maneuver.

Numerical Simulation

The salient features of the computer program developed to perform numerical simulations of the jettison maneuver are associated with numerically integrating the differential equations, iterating for the SM rigid-body accelerations, establishing the logic for the discontinuous boundary conditions, and determining the accuracy requirements for the system of equations.

The numerical integration of the differential equations of motion is accomplished by a fixed-step Runge-Kutta procedure in which the forces and derivatives are recalculated four times during each integration time step.[8] A Runge-Kutta procedure is applicable only to first-order differential equations. Since the equations to be integrated are all second-order differential equations, each second-order equation must be expressed as two first-order equations by a simple change of variables.

Table 1 Typical SM properties at jettison

SM weight	10,650 lb
Oxidizer weight	850 lb
Fuel weight	370 lb
SM centroidal moments of inertia	
I_{xx}	33.14×10^6 lb in.^{2}
I_{yy}	55.88×10^6 lb in.^{2}
I_{zz}	53.74×10^6 lb in.^{2}
I_{xy}	-0.49×10^6 lb in.^{2}
I_{xz}	2.10×10^6 lb in.^{2}
I_{yz}	-2.67×10^6 lb in.^{2}
SM centroid relative to centerline	
y_{cg}	−5.8 in.
z_{cg}	10.9 in.

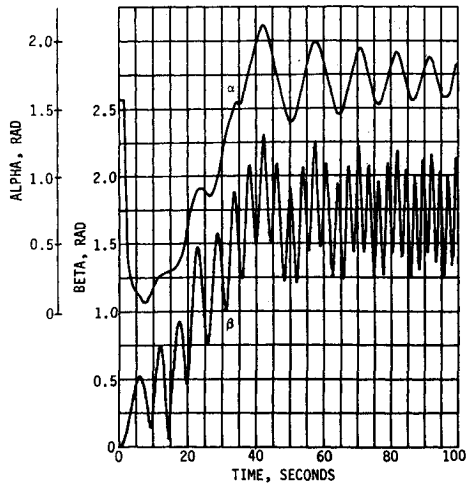

Fig. 7 Orientation angles, α and β.

As previously mentioned, the SM rigid-body acceleration terms appear as contributions to the external forces and moments applied to the SM centroid. This nonlinearity requires that an iteration technique be used to solve for the acceleration terms prior to integration. With the fourth-order Runge-Kutta procedure, the iteration must be performed four times for each integration time step. The initial guesses assumed as acceleration values at the first cycle of a given time point are calculated by linear extrapolation of the converged values from the previous time point. With the initial guesses given, the acceleration terms are calculated and compared with these guesses for convergence. If convergence is not obtained, a new set of guesses is determined for the next pass. A maximum of twenty iteration passes is allowed. During the first ten iterations, the new guesses are set equal to the calculated values. During each of the last ten passes, the new guesses are determined by averaging the calculated values with the guesses used for that pass. Averaging serves to improve convergence by eliminating numerical oscillation. This approach was found to give rapid convergence.

The derived system of equations allows for the propellant masses to impact with and to separate from the tank walls. To represent the inelastic impact, which involves discontinuous fluid motion and instantaneous energy loss, the local relative radial velocity and acceleration are set to zero when the radial position coordinate equals the tank radius. To represent the separation from the tank wall, the forces applied to the propellant mass are set to zero when the radial position coordinate is less than the tank radius or when the normal constraint force applied to the point mass is tensile.

Since the motion of a propellant mass is described by different variables depending on whether it is located in the forward, central, or aft sections of its tank, a change of variables must be performed when a location change occurs. Based on requirements for numerical accuracy, the procedure that evolved is to predict continuously the time at which each fluid changes location. Then, when one of these times becomes less than the constant integration time step, the program integrates to the location change, performs the change of variables, and completes integration of that time step.

Table 2 Preset RCS firing sequence

Time	Event
$t = 0$	RCS $-x$ thrust begins (100 lb/thruster)
$t = 0.1$	SM–CM separation
$t = 2.0$	RCS roll jets fire
$t = 7.5$	RCS roll jets off
$t \simeq 300$	RCS $-x$ thrust terminates

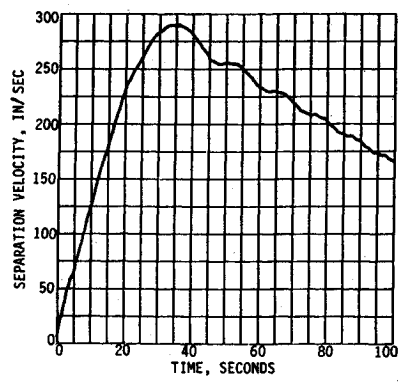

Fig. 8 Service module separation velocity.

The equations for the propellant motions are extremely sensitive; and the necessity for double precision arithmetic was readily identified from the results of a check for conservation of energy. Even with double precision (16 digits on the SRU 1108 computer), the maximum integration time step allowed by the propellant motions is 0.005 sec. In addition, the singularities associated with the use of spherical and cylindrical local coordinates require special attention. Whenever the solution approaches within a given distance of a singularity, the integration time step is automatically decreased an order of magnitude to maintain numerical stability. Numerous test simulations for specialized conditions increased confidence in the numerical stability of the calculations and in the accuracy and repeatability of the results.

Results

For convenience in approximating the *relative* motion between the Command and Service Modules, the origin of the inertial coordinate system is assumed to be moving with the CM at constant inertial velocity. Typical SM mass properties are shown in Table 1. A damping coefficient C_F of 0.01 was used in Eqs. (18–21) to represent the propellant damping. This analytical value was obtained from the classical solution of the energy losses for turbulent fluid flow in curved pipes.

Ten SM jettison simulations were made by varying the magnitude of the propellant masses and their initial position within the tanks. The RCS firing sequence used was the sequence employed during the flights of Apollo 7–12 as shown in Table 2. Five of the ten simulations indicated the possibility of retrograde motion. SM and propellant response time histories for a case exhibiting retrograde motion are shown in Figs. 5–9. In this example, the SM demonstrates flight characteristics suggestive of a boomerang and, after 400 sec of flight, passes within about 400 ft of the CM.

The following is a brief description of the complex interaction between the SM motion and the motion of the fluids within the tanks. During the first two seconds after separation, the propellants move to the forward ends of the tanks under the action of the $-x$ RCS thrusters (Fig. 5). During this same time, the SM rotates slightly about the y and z

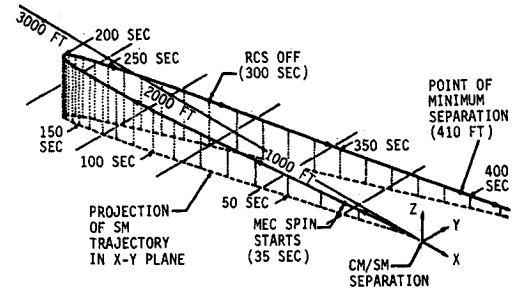

Fig. 9 Service module separation trajectory relative to command module.

axes primarily because of the moments resulting from the offset SM centroid (Fig. 6). Then, with the initiation of $+x$ roll at $t = 2.0$ sec, the propellants are forced to the outer envelope of the tanks. The propellant forces and unsymmetric SM mass properties cause a wobble about the inertial X axis which excites longitudinal motion of the propellants in the tanks (Fig. 5). At termination of the roll-jet firing ($t = 7.5$ sec), the SM has attained a spinning motion similar to the desired spin-stabilized attitude (Fig. 6a). However, the gross longitudinal sloshing of the propellants persists, and the energy dissipation resulting from this fluid motion ultimately results in the SM rotating about its axis of maximum moment of inertia. This is because a rotating body, capable of dissipating energy internally, tends to assume a configuration which is stable and which has the minimum kinetic energy.

Since the desired spin-stabilized attitude of the SM is not the attitude of minimum energy, the SM spinning motion tends toward the minimum energy configuration (MEC) with α, the angle between the rotational velocity vector and the body x axis, oscillating about a value near 90° (Fig. 7). The angle β between the body x axis and the inertial X axis also oscillates about a value near 90° (Fig. 7). As the SM enters the MEC spin, the propellants are forced to the forward or aft ends of the tanks where they remain. Thus the MEC is a stable configuration. The position of the propellants and the location of the SM centroid determine the mean values of α and β. If the mean value of β is greater than 90°, the $-x$ RCS force will have a component in the positive inertial X direction which decreases the relative separation velocity between the SM and CM (Fig. 8). Then, if the RCS thrust remains on long enough, the SM will finally attain a retrograde velocity and may pass close to the CM as shown in Fig. 9. With a mean value of β less than 90°, the SM will retain a force component in the $-X$ direction providing additional separation velocity.

Concluding Remarks

As demonstrated by the preceding analytical results, gross propellant slosh or fluid reorientation can have significant effects on the motions of a spacecraft in a low-g environment. To represent this phenomenon adequately, the propellant motion must be described by general equations rather than by the more restrictive spring-mass slosh equations. Since these general equations are very sensitive to numerical inaccuracies, extreme care is required in their solution.

The motion of the SM during jettison is influenced by the damping characteristics of the propellants. Although some studies of low-g slosh have been made,[9,10,11] energy dissipation during fluid reorientation in a low g environment is not well defined.

References

[1] Kincade, R. E., "Summary of SM Entry for Apollo Missions 7, 8, 9, 10 and 11," 69-FM37-323, Aug. 1969, NASA.

[2] Britton, E. R., "Investigation—Service Module Entry Problem," SD69-631, Oct. 1969, North American Rockwell Corp., Downey, Calif.

[3] Rothrock, J. E., "Service Module Stability Study," 5524.8-99, Sept. 1969, TRW Controls Corp., Houston, Texas.

[4] Merchant, D. H. and Gates, R. M., "CM-SM Separation Dynamics," 5-2961-HOU-107, Dec. 1969, The Boeing Co., Houston, Texas.

[5] Gates, R. M. and Merchant, D. H., "General Motion of a Rigid Spacecraft with Fluid Reorientation—Theoretical Manual," D2-118301-1, May 1970, The Boeing Co., Houston, Texas.

[6] Murray, J. F., "General Motion of a Rigid Spacecraft with Fluid Reorientation—Computer User's Manual," D2-118301-2, May 1970, The Boeing Co., Houston, Texas.

[7] Synge, J. L. and Griffith, B. A., *Principles of Mechanics*, 3rd ed., McGraw-Hill, New York, 1959, pp. 428–429.

[8] Milne, W. E., *Numerical Solution of Differential Equations*, Wiley, New York, 1953, pp. 72–73.

[9] Stephens, D. G., "Experimental Investigation of Liquid Impact in a Model Propellant Tank," TN D-2913, 1965, NASA.

[10] Abramson, H. N., ed., *The Dynamic Behavior of Liquids in Moving Containers*, NASA SP-106, 1966.

[11] Dodge, F. T. and Garza, L. R., "Simulated Low-Gravity Sloshing in Spherical, Ellipsoidal, and Cylindrical Tanks," *Journal of Spacecraft and Rockets*, Vol. 7, No. 2, Feb. 1970, pp. 204–206.